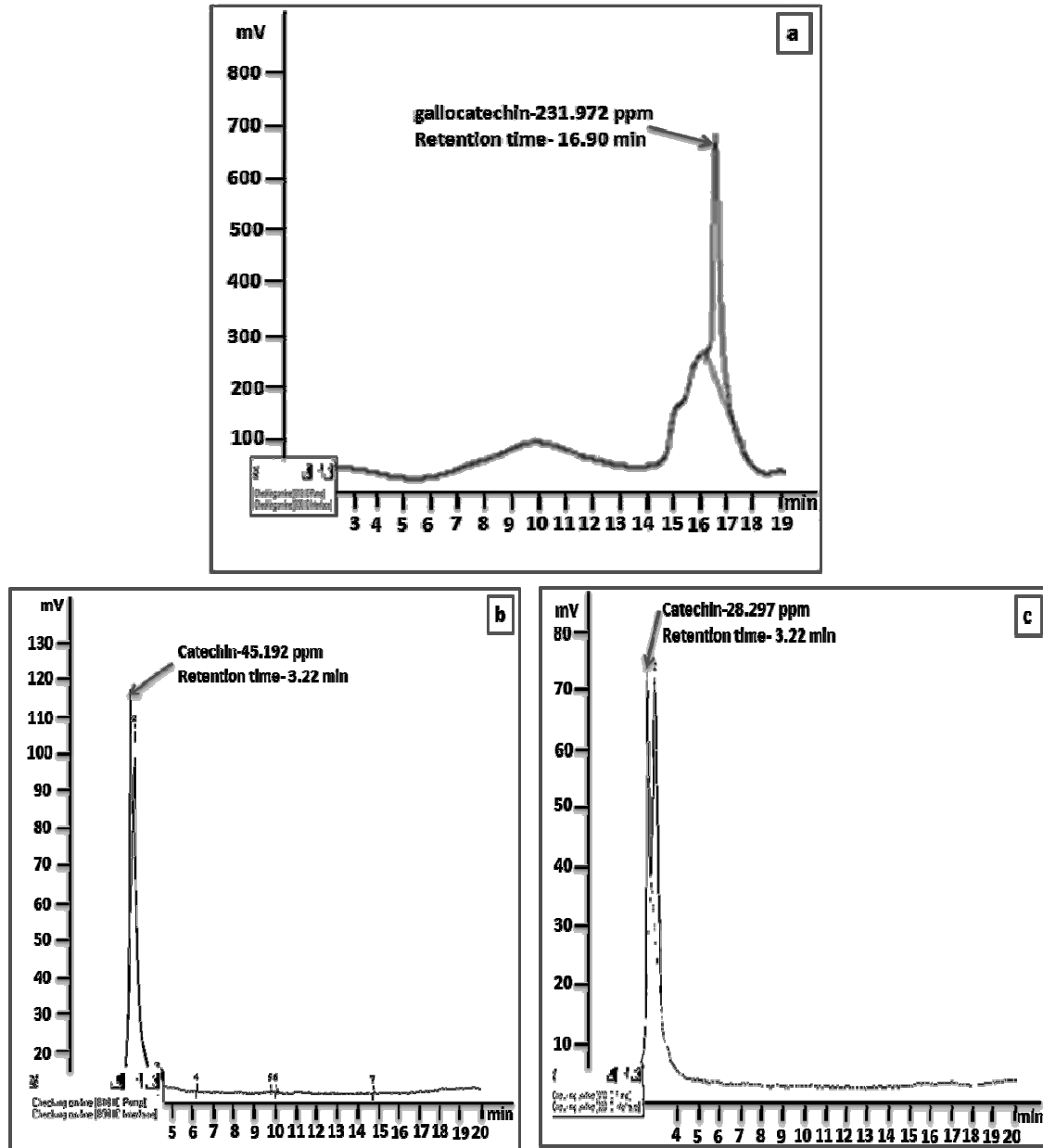


Banana fruits, *Musa Paradisica*, are a rich source of vitamins and nutrients and consumed industrially throughout the world. However, the peels of the fruits are not used by people or any industry. These unutilized peels constitute health risks for humans after ripening [Montelongo et al., 2009]. But, it is an interesting fact that banana peels contain higher content of nutrients than banana pulp [Davey et al., 2007]. In addition, to use banana peels as a corrosion inhibitor will be economical as well as eco-friendly. So, we have selected banana peels for corrosion inhibition studies. We have investigated the effect of banana peels as well as the effect of ripening of the peels on mild steel corrosion in HCl and H<sub>2</sub>SO<sub>4</sub> media by weight loss method, Tafel polarization curves, EIS, FTIR spectroscopy, UV-visible Spectroscopy, and AFM techniques. The results are summarized and discussed under following sections.

### **5.1 Characterization of *Musa Paradisica* Peel Extracts**

#### *HPLC Study:*

Figure 41 shows HPLC chromatographs of raw, ripe and over ripe banana peel extract. Various peaks could be observed in the graphs, which showed presence of different organic compounds in the extracts. But, we have identified only the major constituent of the extracts. In the chromatograph of raw banana peels, a major compound was identified at the retention time of 16.90 minute. The compound corresponded to the standard retention time of gallicocatechin. The concentration of gallicocatechin was found as 231.972 ppm. Other scientists have also reported gallicocatechin from banana peels, which validate our results [Someya et al., 2002; Sundaram et al., 2011]. As gallicocatechin is the chief organic compound of raw banana peel extract, it can be stated that inhibition potential of the extract depends on the performance of gallicocatechin.



**Figure 5.1** HPLC graphs of (a) RMPPE, (b) RIMPPE and (c) ORIMPPE

The effect of ripening of the peels was also studied by HPLC technique. In ripe and over ripe banana peel extract, an intense peak was obtained at retention time of 3.22 minute while peak at 16.90 min was not observed. This indicated that gallocatechin was not present in other extracts. The major compound of ripe and over ripe banana peel extract was detected as catechin; however, the content of catechin varied in ripe (45.192 ppm) and over ripe (28.197ppm)

banana peel extract. On the basis of above discussion, it could be stated that gallic catechin was gradually degraded with maturity of the peels. Possibly, gallic catechin transformed into some other unstable organic molecules and released catechin along with other by products on further oxidation. The content of catechin in over ripe banana peel extract was found lesser than the content of catechin in ripe banana peel extract. This fact confirmed the degradation of bioactive compounds of the extracts with ripening of banana peels.

*UV-Visible Spectroscopy:*

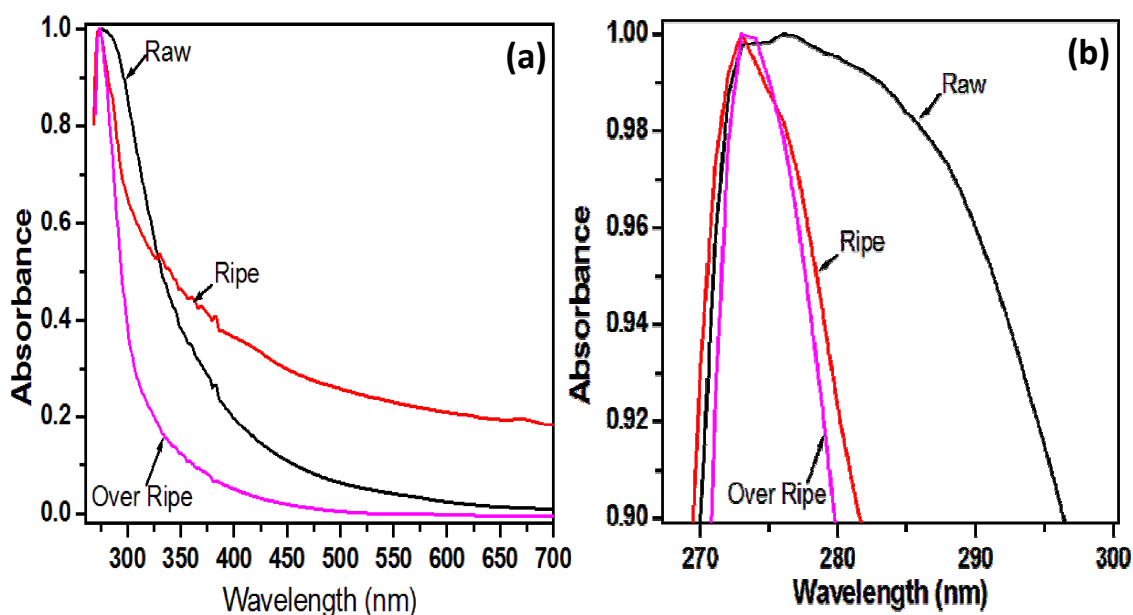


**Figure 5.2 UV-visible spectra of (a) banana peel extracts and (b). Zoom in view of the spectra.**

UV-visible spectra of banana peel extracts are shown in Figure 42a. From Figure 42 a peak at 274 nm could be observed in the spectrum of all the extracts, suggesting that gallic catechin was present in the extracts [Miketova et al., 2000]. However, it was noticed that the nature of peaks changed with ripening of the extracts. A broad peak was obtained for RMPPE while a sharp peak was acknowledged for other two extracts (Figure 42b). This showed that raw banana peels were containing some organic compounds that were

absent in ripe and over ripe banana peels. In view of these facts, it could be stated that that RMPPE possessed higher content of bioactive compounds before ripening, which was gradually degraded with the maturity period. Other scientists have also reported the information similar to our findings [Nguyen et al., 2003; Wang and Jiao, 2001]. In addition, this fact could be clearly observed by HPLC chromatographs of the extracts.

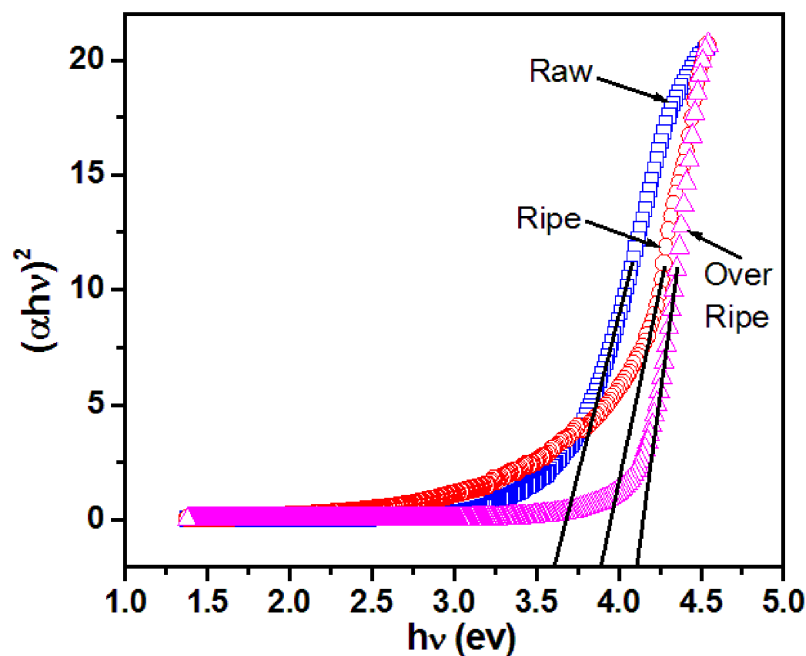


**Figure 5.3 Showing Band gap of banana peel extracts**

To further explore the data provided by UV-Visible spectra, the optical band gap of the extracts matters was determined using the following relationship [Singh et al., 2009]:

$$\alpha hv = B(hv - E_g)^n \quad (26)$$

where  $\alpha$  is an absorption coefficient,  $h\nu$  is the photonic energy of absorbed light,  $E_g$  is the optical band gap of substance and  $B$  is a proportionality constant. The optical band gap of the extracts matters was determined by a graph plotted between  $(\alpha hv)^2$  and  $h\nu$  values. The linear

segment of the curves was extrapolated to zero as demonstrated in Figure 43 and  $E_g$  has been obtained. From Figure 43 it is obvious that the band gap value of the extracts organic matters was changed with ripening of the peels. This fact indicated the molecular changes in the extracts constituents during maturity ages of the peels. The reason of the change in band gap of the material could be given as degradation of the bioactive compounds of the extracts with the ripening time. This statement was well supported by HPLC study and UV-Visible spectroscopy. The band gap of the extracts does not have any real meaning; however, the study is able to show the molecular changes during different maturity ages of banana peels.

*FTIR Spectroscopy:*

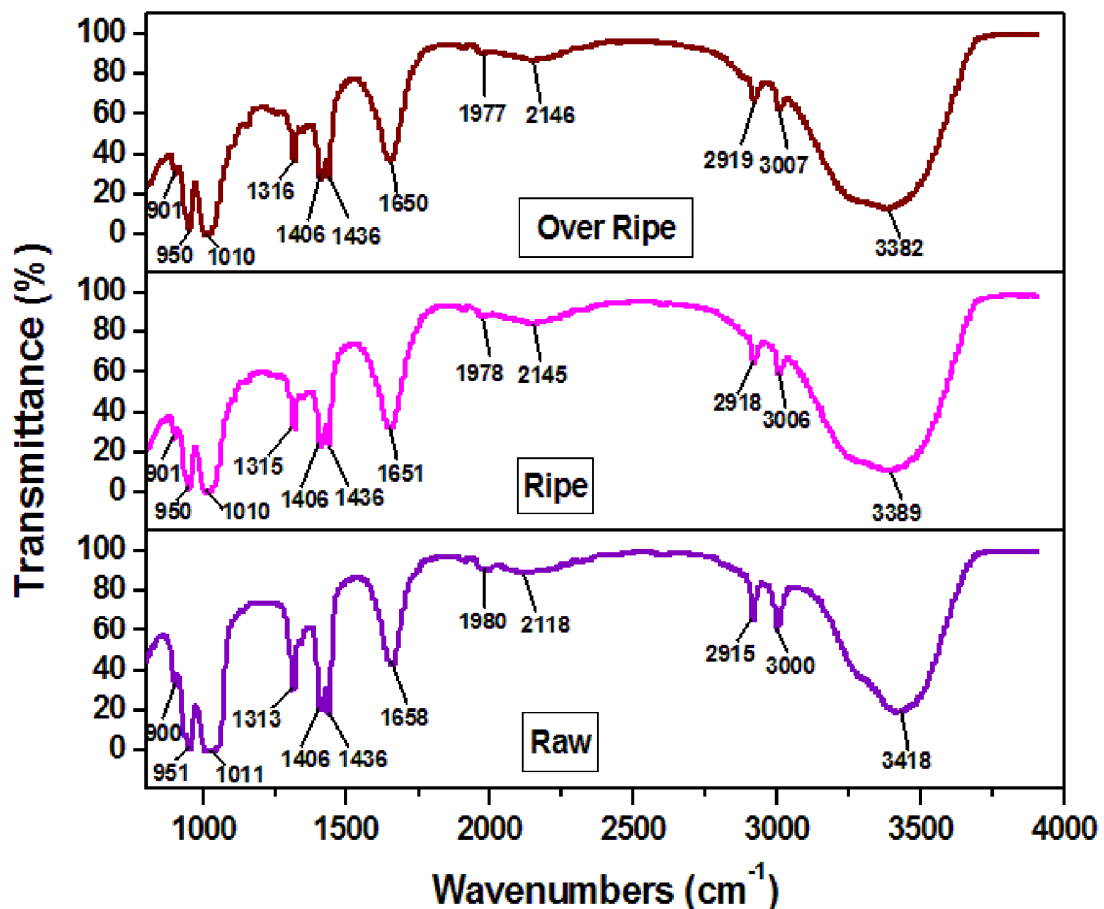


Figure 5.4 FTIR spectra of banana peel extracts at different maturity stages

FTIR spectra of raw, ripe and over ripe banana peel extracts are illustrated in Figure 44. Careful inspection of the spectra revealed that all the extracts had similarity in peaks positions, but showed a clear difference in intensity of peaks. However, the difference in intensities was more effectively visualized for raw and ripe extract with respect to ripe and over ripe extract. A decrease in intensity of the peaks with ripening of banana peels suggested that organic matters of the extract degraded with maturity of the peels. This fact is well supported by UV-visible and HPLC study.

A strong and broad absorption band at 3382/3389/3418  $\text{cm}^{-1}$  is observed in the spectra due to O-H or N-H stretching vibration. Two small peaks at 2915/2918/2919  $\text{cm}^{-1}$  and 3000/3006/3007  $\text{cm}^{-1}$  can be attributed to C-H stretching frequencies. A small band at 2118  $\text{cm}^{-1}$  can be related to  $\text{C} \equiv \text{C}$  stretching frequency. A medium peak at 1658  $\text{cm}^{-1}$  reflect C=C and C=N stretching or N-H bending vibrations. The C-H and O-H bending vibrations can be noticed at 1406 and 1436  $\text{cm}^{-1}$ , respectively. The absorption band at 1316  $\text{cm}^{-1}$  can be attributed to C-N stretching vibration, and the peak at 1010  $\text{cm}^{-1}$  can be related to C-O stretching vibration. A small peak at 950  $\text{cm}^{-1}$  indicates C-H or C-O stretching frequencies of functional groups. Thus, results have demonstrated that banana peels extracts contain organic moieties that have oxygen and nitrogen atoms along with aromatic rings, which fulfill the fundamental requirements of a good corrosion inhibitor.

### 5.2 Weight Loss Experiments

Figure 45 demonstrates the effect of concentration of the extracts on mild steel corrosion in 1 M HCl. From careful inspection of Figure 45 it was revealed that that an increase in inhibitor concentration caused decrease in corrosion rate but increase in inhibition efficiency. With the

increase in inhibitor concentration, surface area of mild steel was more effectively blanketed by organic molecules of the extracts. Thus, enhanced corrosion inhibition of mild steel was acknowledged. However, no significant corrosion inhibition activity was acknowledged beyond  $300 \text{ mg L}^{-1}$  concentration of the extracts, which probably occurred due to saturated adsorption rate of inhibitor on mild steel surface. Furthermore, it could be clearly observed from weight loss study that inhibition efficiency of the extracts decreased with the maturity of banana peels and followed the order: Raw > Ripe > Over Ripe. A maximum corrosion inhibition of 92 % was acknowledged using RMPPE, while RIMPPE and ORIMPPE provided 84% 79% inhibition efficiency respectively. The reason of this fact could be given as degradation or decomposition of chemical constituents of banana peels with ripening of the fruits (UV-vis, HPLC and FTIR study), which affected molecular adsorption rate of inhibitor on mild steel.

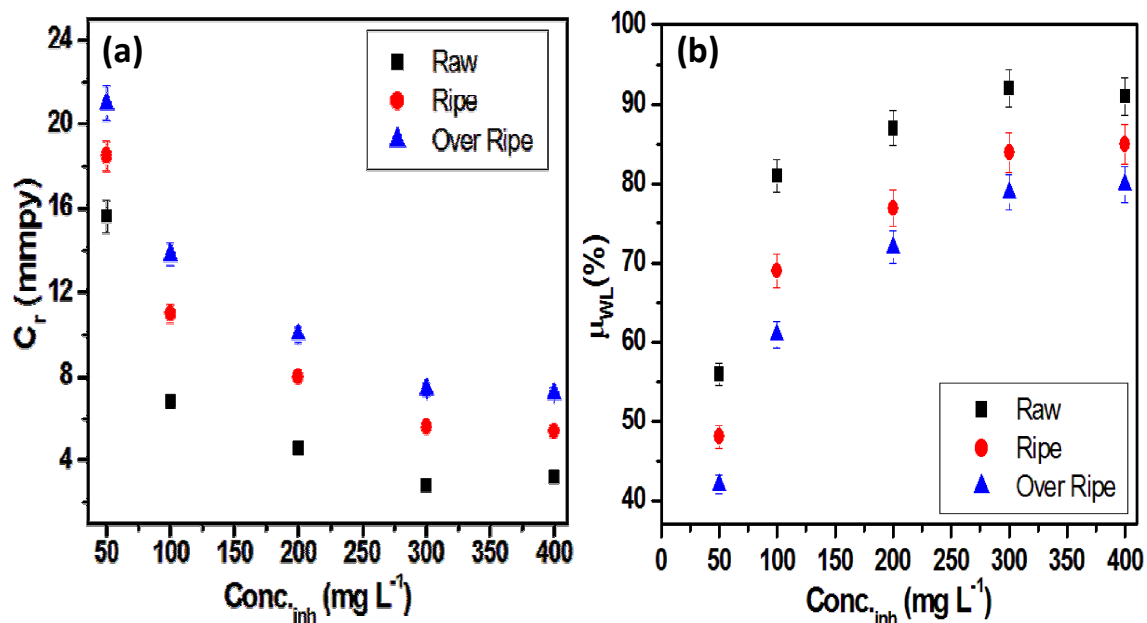


**Figure 5.5 Corrosion rates and Inhibition efficiencies obtained by weight loss method in 1 M HCl at different concentrations of banana peel extracts at  $26 \pm 1^\circ \text{C}$**

The behavior of mild steel in  $\text{H}_2\text{SO}_4$  in presence of banana peel extracts was found similar to that in HCl solution. The inhibition efficiency of the extracts increased with the

concentration while corrosion rate decreased (Table 11). A maximum inhibition efficiency of 86%, 78% and 72% was achieved using raw, ripe and over ripe banana peel extract, respectively. The inhibition efficiencies in HCl were found more than their corresponding values in H<sub>2</sub>SO<sub>4</sub>, which suggested that adsorption of inhibitor molecules on steel was more convenient in hydrochloric acid with respect to sulfuric acid.

**Table 5.1 Corrosion rate and inhibition efficiency values for mild steel in 0.5 H<sub>2</sub>SO<sub>4</sub> obtained by weight loss method at 26± 1°C**

Type of extract	Conc. of Inhibitor	Weight loss (mg cm <sup>-2</sup> )	Inhibition efficiency $\mu_{WL}$ (%)	Corrosion rate (C <sub>r</sub> ) (mmpy)	Surface Coverage ( $\theta$ )	C / $\theta$ (mg L <sup>-1</sup> )
	blank	20.4	-	45.7	-	-
<b>Raw</b>	50 mg L <sup>-1</sup>	10.4	49	23.3	0.49	102
	100 mg L <sup>-1</sup>	5.1	75	11.4	0.75	133
	200 mg L <sup>-1</sup>	4.1	80	9.1	0.80	250
	300 mg L <sup>-1</sup>	2.9	86	6.5	0.86	348
	400 mg L <sup>-1</sup>	3.3	84	7.4	0.84	476
<b>Ripe</b>	50 mg L <sup>-1</sup>	9.8	42	21.9	0.42	119
	100 mg L <sup>-1</sup>	7.9	61	17.8	0.61	163
	200 mg L <sup>-1</sup>	6.1	70	13.7	0.70	285
	300 mg L <sup>-1</sup>	4.5	78	10.1	0.78	385
	400 mg L <sup>-1</sup>	4.5	78	10.1	0.78	512
<b>Over Ripe</b>	50 mg L <sup>-1</sup>	13.5	34	30.1	0.34	147
	100 mg L <sup>-1</sup>	8.8	53	19.6	0.53	188
	200 mg L <sup>-1</sup>	7.3	64	16.4	0.64	312
	300 mg L <sup>-1</sup>	5.9	71	13.2	0.71	422
	400 mg L <sup>-1</sup>	5.7	72	12.7	0.72	555

### 5.2.1 Adsorption Isotherms

Figure 46 shows UV-visible spectra of adsorbed inhibitor molecules on iron surface in HCl and H<sub>2</sub>SO<sub>4</sub> solutions. Careful inspection of Figure 46 revealed that both spectra was having pattern similar to pure extract. This indicated that chemical constituents of the extracts were adsorbed on the metal surface in both acid media.

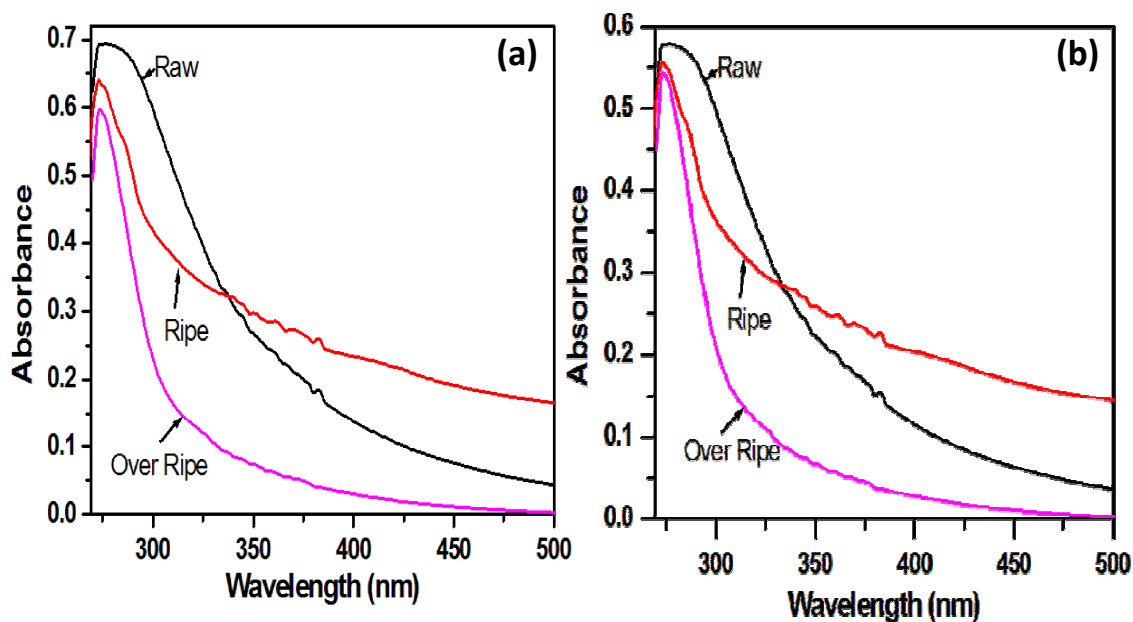


**Figure 5.6** UV-Visible spectra of solutions containing washing of mild steel immersed in (a) 1 M HCl and (b) 0.5 M H<sub>2</sub>SO<sub>4</sub> in presence of inhibitors (300 mg L<sup>-1</sup>)

Furthermore, adsorption characteristics of banana peel extracts were investigated by various adsorption isotherms. However, we obtained best fitting results by Langmuir isotherm in both acid solutions. The values of regression coefficient  $R^2$  (given in Figure 47) and slope of the straight lines (raw-1.01, ripe- 1.05 and over ripe-1.08) were equivalent to one, showing accuracy of the selection. Further investigation of adsorption parameters revealed that  $K_{ads}$  values decreased with maturity of banana peels in both acid media. This meant that the organic matters of RMPPE were more effectively adsorbed on mild steel surface than organic molecules of RIMPPE and ORIMPPE. In addition, it was also observed

that  $K_{ads}$  values were higher in HCl than  $H_2SO_4$ , which indicate that molecular adsorption of inhibitor was more effective in hydrochloric acid with respect to sulfuric acid. Hence, better corrosion inhibition was acknowledged in HCl.

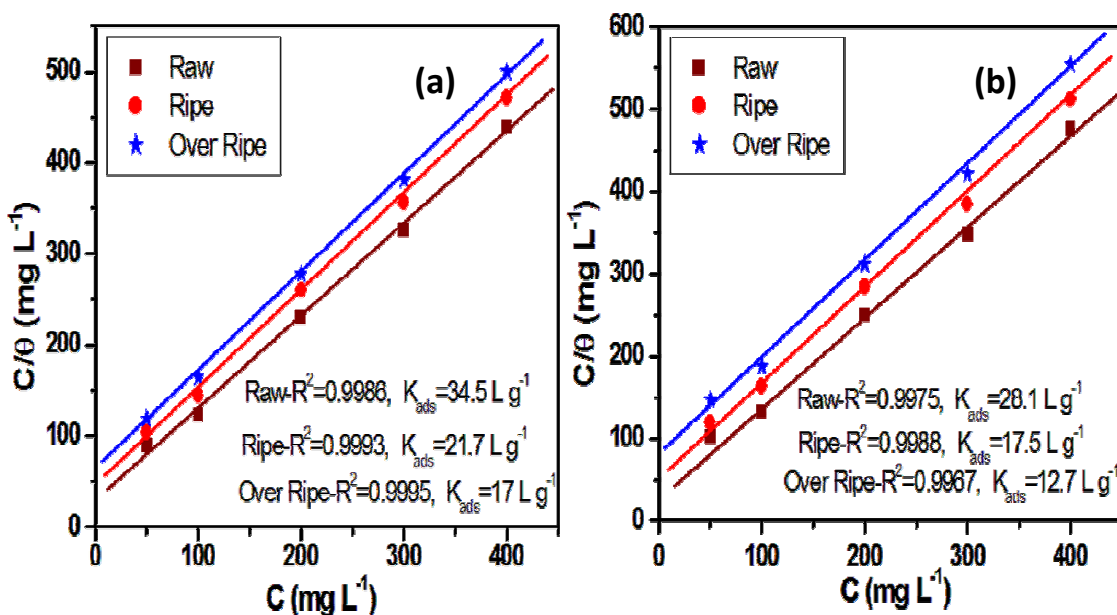


Figure 5.7 Langmuir isotherm fitting for mild steel in (a) 1 M HCl and (b) 0.5 M  $H_2SO_4$  at room temperature.

### 5.2.2 Effect of Immersion Time

Figure 48 demonstrates the effect of immersion time (120 hours) on mild steel corrosion rate in 1 M HCl and 0.5 M  $H_2SO_4$  in presence of banana peel extracts (300 mg L<sup>-1</sup>). Careful inspection of Figure 48 revealed that corrosion rate in blank HCl increased sharply to 66 hours and became saturated for rest of the test period, while a remarkable control on corrosion rate could be clearly observed in Figure 48. Similar behavior of mild steel corrosion was acknowledged in sulfuric acid. However, a slight acceleration in mild steel corrosion was obtained with immersion time and type of the extracts in both acid media, which indicated degradation/desorption of inhibitor molecules with the changes in parameters [Bentiss et al., 2005, Oguzie et al., 2012]. The reason of enhanced corrosion

resistance of mild steel in HCl and H<sub>2</sub>SO<sub>4</sub> could be attributed to the high stability of the adsorbed inhibitor molecules, which formed a protective barrier over mild steel surface and restricted the access of corrosive molecules for long time. Furthermore, it was revealed from test results that the extracts performance was more effective in hydrochloric acid than sulfuric acid. The reason of this fact could be given as higher adsorption rate and/or lower desorption rate of the extract molecules in HCl in comparison to H<sub>2</sub>SO<sub>4</sub>.

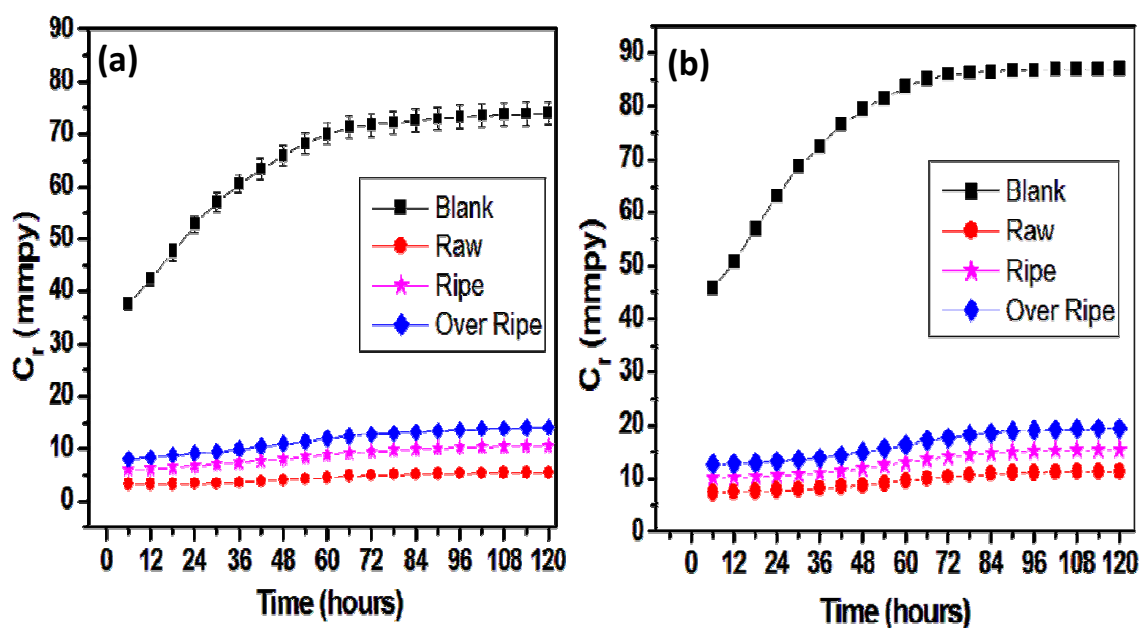


Figure 5.8 Showing effect of immersion time on inhibition potential ( $300 \text{ mg L}^{-1}$ ) of the extracts in (a) 1 M HCl and (b) 0.5 M H<sub>2</sub>SO<sub>4</sub> at room temperature for 120 Hours.

### 5.2.3 Effect of Acid Concentration on Inhibition Potential of Extracts

Figure 49 illustrates the effect of change in acid concentration on inhibition efficiency and corrosion rate values of  $300 \text{ mg L}^{-1}$  raw, ripe and over ripe banana peel extracts. Figure 49 revealed that corrosion rate of mild steel increased with increase in HCl concentration, while inhibition efficiency decreased with the acid concentration.

Maximum increase in corrosion rate/decrease in inhibition efficiency was acknowledged for over ripe banana peel extracts whereas minimum damage to mild steel was observed in HCl with raw banana peel extract. Similar results were achieved in  $H_2SO_4$  solutions (Figure 49b). However, higher inhibition efficiency of the extracts was acknowledged in HCl than  $H_2SO_4$ .

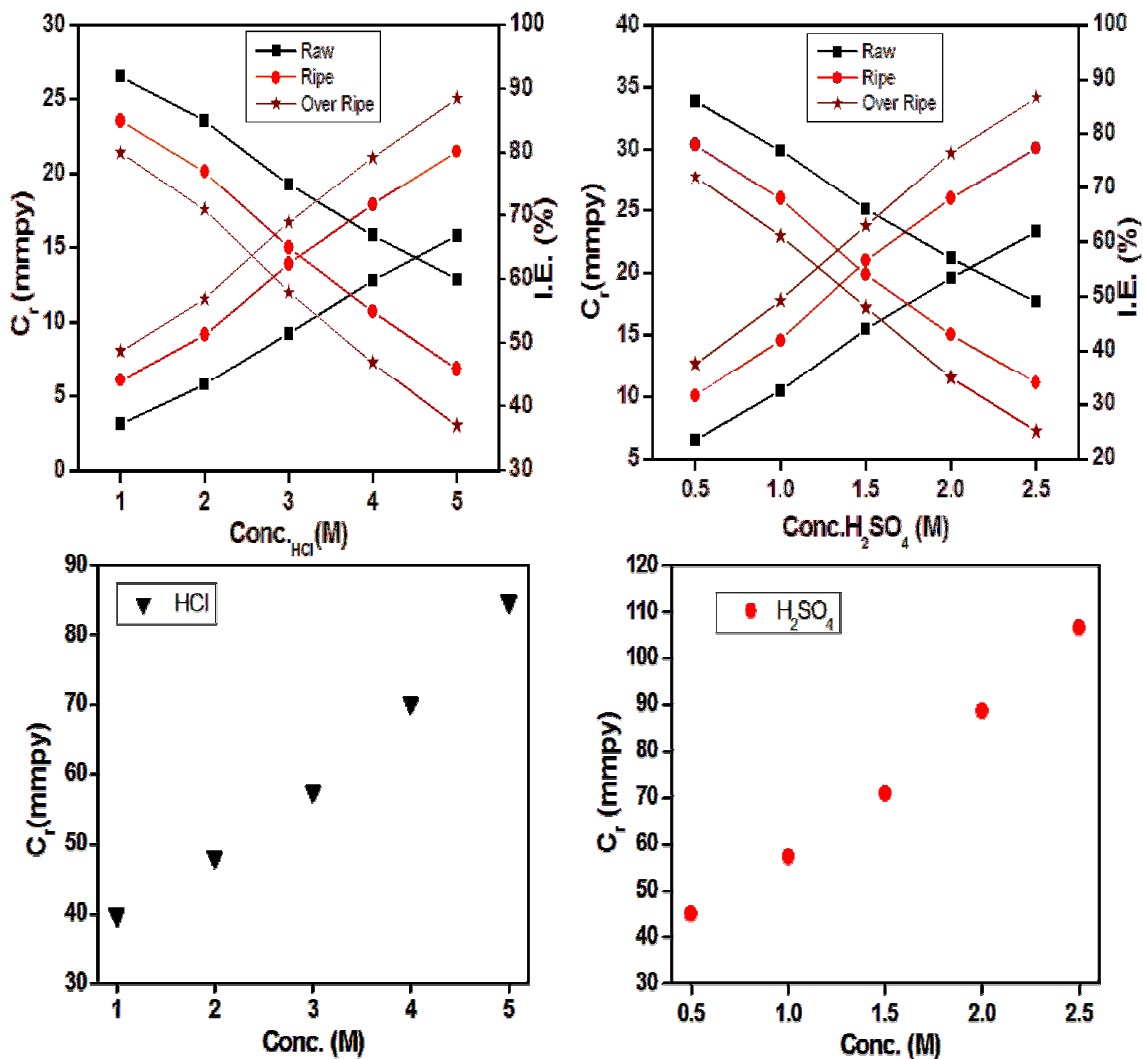


Figure 5.9 Showing the effect of the concentrations of HCl and  $H_2SO_4$  on corrosion rates and inhibition efficiencies

The decrease in corrosion protection ability of the extracts with increase in concentration of both acid media could be attributed to either high rate of desorption of inhibitor

molecules from the metal surface or low adsorption rate of extract molecules from solution to metal surface [Mathur and Vasudevan, 1982].

#### 5.2.4 Effect of Temperature on Corrosion Inhibition

The effect of temperature rise (30°-60° C) on inhibitory action of banana peel extracts in 1 M HCl and 0.5 M H<sub>2</sub>SO<sub>4</sub> has been investigated and shown in Figure 50. It was observed through inspection of Figure 50 that the values of slope and intercept of straight fitting lines increased with the inhibitor concentration in both acid solutions. This fact suggested that the energy of activation and Arrhenius coefficient of mild steel corrosion process enhanced in presence of banana peel extracts, indicating that the extract molecules were adsorbed on mild steel surface through electrostatic interaction (Physical adsorption) [Martinez and Stern, 2002]. The values of  $E_a$  and  $A$  was found maximum for raw banana peel extract and minimum for over ripe banana peel extract. Also, bigger values of activation energy and Arrhenius coefficient were achieved in HCl than in H<sub>2</sub>SO<sub>4</sub>. Hence, it could be concluded from inspection of above mentioned facts that presence of inhibitor raised the minimum energy limit of inhibitive barrier at metal-acid interface and hence corrosion inhibition occurred.

Attempts were made to plot a graph between  $C_r/T$  and  $1/T$  values for mild steel in HCl and H<sub>2</sub>SO<sub>4</sub> solutions. According to Transition state equation (Eq. 19) it is evident that the slopes of lines provides the values of enthalpy ( $\Delta H^*$ ) of activation while intercepts gives the values of entropy ( $\Delta S^*$ ) of activation. Accordingly,  $\Delta H^*$  and  $\Delta S^*$  values were calculated by the slopes and intercepts of fitting lines and listed in Table 12. A careful investigation of the results mentioned in Table 12 and Figure 51 revealed that the  $\Delta H^*$  values of inhibited mild steel were positive as well as greater than the values of corroded

sample. This observation indicated that the value of energy to corrode mild steel rose with the extract concentration, suggesting that the protective barrier of inhibitor molecules made mild steel corrosion difficult for acid solutions in presence of the extract [Mu et al., 2004]. The maximum value of  $\Delta H^*$  was achieved using raw banana peel extract while the lowest value was acknowledged for over ripe banana peel extract, which showed better thermal stability of RMPPE than other studied extracts. In addition,  $\Delta H^*$  values were higher in HCl in comparison to the values in  $H_2SO_4$  showing that that the extracts performed more effectively in hydrochloric acid than sulfuric acid. Furthermore, the results showed a well known relation (Eq. 22) between  $\Delta H^*$  and  $E_a$  in both acid media, which verified the outcome of thermo gravimetric experiments.

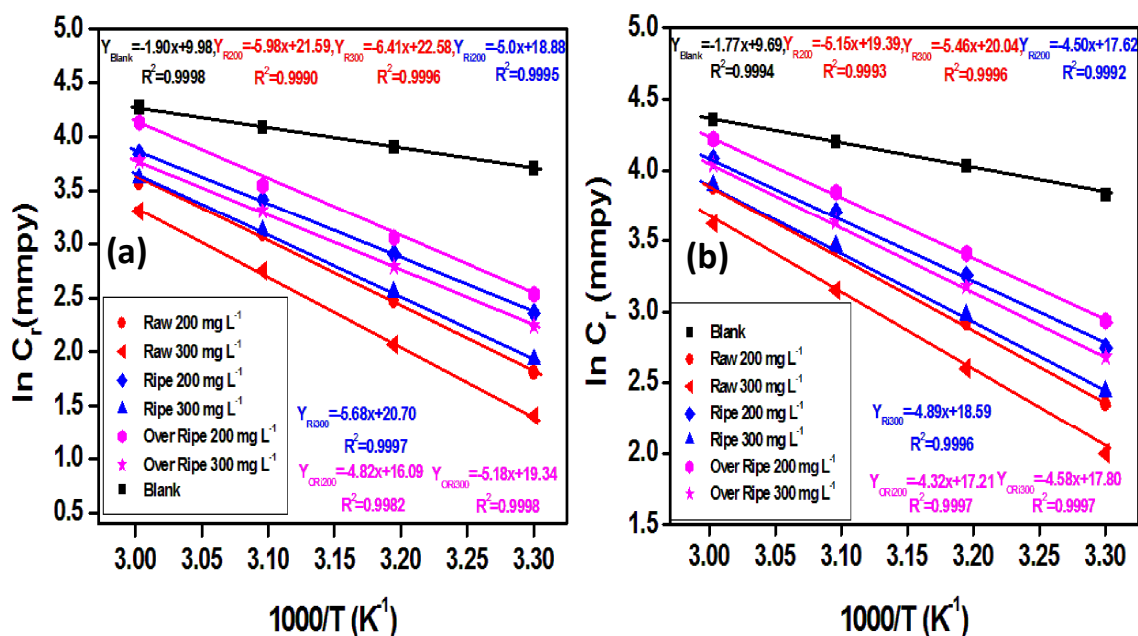


**Figure 5.10** Arrhenius plot for mild steel in (a) 1 M HCl and (b) 0.5 M  $H_2SO_4$  with different concentrations of Banana Peel Extracts

It was revealed from Table 12 that randomness of the system  $\Delta S^*$  increased with increase in the extract concentration. The maximum increase in  $\Delta S^*$  values were obtained for

RMPPE while minimum values were acknowledged for ORIMPPE in both acid media. Possibly, the reactants were transformed into activated complex during the reaction, which might happen due to adsorption of the extract molecules over metal surface [Sahin et al., 2002]. Basically, the molecular adsorption of the organic moieties on metals in aqueous solutions is a type of quasi-substitution interactions between water and inhibitor molecules. Thus, it could be explained via above mentioned theory that the inhibitor molecules replaced water molecules adsorbed on the metal surface in corrosion inhibition process. Consequently,  $\Delta S^*$  values increased with the extract concentration, which might occur as a result of increase in entropy of the solvent with increase in inhibitor concentration. Furthermore, the higher values of  $\Delta S^*$  were achieved in HCl than  $H_2SO_4$  medium indicating that the effect of banana peel extracts on corrosion of mild steel was more prominent in hydrochloric acid in comparison to sulfuric acid.

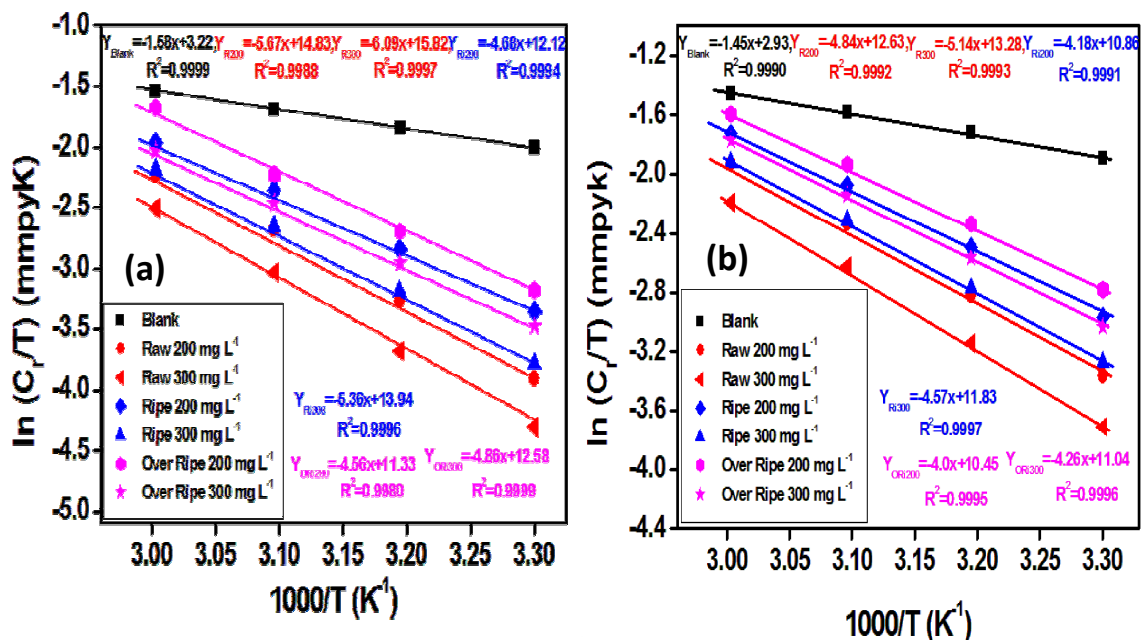


Figure 5.11 Transition state plots for mild steel in (a) 1 M HCl and (b) 0.5 M  $H_2SO_4$  with different concentrations of Banana Peel Extracts

**Table 5.2 Activation parameters for mild steel in 1 M HCl without and with different concentrations of CBRE**

Acid solution	Conc. of Inhibitor (mg L <sup>-1</sup> )	A (mmpy)	E <sub>a</sub> (kJ mol <sup>-1</sup> )	ΔH* (kJ mol <sup>-1</sup> )	ΔS* (J mol <sup>-1</sup> K <sup>-1</sup> )	E <sub>a</sub> - ΔH* (kJ mol <sup>-1</sup> )
<b>HCl</b>	Blank	2.25 × 10 <sup>4</sup>	15.79	13.13	-170.68	2.66
	Ra <sub>200</sub>	2.61 × 10 <sup>9</sup>	49.79	47.14	-74.16	2.65
	Ra <sub>300</sub>	7.05 × 10 <sup>9</sup>	53.29	50.63	-65.93	2.66
	Ri <sub>200</sub>	1.71 × 10 <sup>8</sup>	41.57	38.91	-96.69	2.66
	Ri <sub>300</sub>	1.06 × 10 <sup>9</sup>	47.22	44.56	-81.56	2.65
	ORi <sub>200</sub>	1.04 × 10 <sup>7</sup>	40.02	37.37	-103.25	2.65
	ORi <sub>300</sub>	2.72 × 10 <sup>8</sup>	43.06	40.40	-92.86	2.66
<b>H<sub>2</sub>SO<sub>4</sub></b>	Blank	1.68 × 10 <sup>4</sup>	14.71	12.05	-173.09	2.66
	Ra <sub>200</sub>	2.86 × 10 <sup>8</sup>	42.81	40.15	-92.45	2.65
	Ra <sub>300</sub>	5.50 × 10 <sup>8</sup>	45.39	42.73	-87.04	2.66
	Ri <sub>200</sub>	4.84 × 10 <sup>7</sup>	37.41	34.75	-107.16	2.66
	Ri <sub>300</sub>	1.28 × 10 <sup>8</sup>	40.65	37.99	-99.10	2.66
	ORi <sub>200</sub>	3.20 × 10 <sup>7</sup>	35.91	33.25	-110.57	2.66
	ORi <sub>300</sub>	5.8 × 10 <sup>7</sup>	38.07	35.42	-105.67	2.65

### 5.3 Tafel Potentiodynamic Polarization Study

The polarization behavior of mild steel in 1 M HCl and 0.5 H<sub>2</sub>SO<sub>4</sub> in absence and presence of the extracts has been investigated and shown in Figure 52 and 53. From careful inspection of polarization curves shown in Figure 52 and 53, it was revealed that the increase in inhibitor concentration caused a shift in equilibrium corrosion potential (E<sub>corr</sub>) and reduction in corrosion current (I<sub>corr</sub>). This behavior showed retarded corrosion of mild steel in acid media in presence of inhibitors. Furthermore, it could be clearly

observed from Figure 52 and 53 that adsorption of organic molecules of the extracts affected both anodic and cathodic reactions, which indicated the mixed type corrosion inhibition in both acid media [Ferreira et al., 2004; Li et al., 2008].

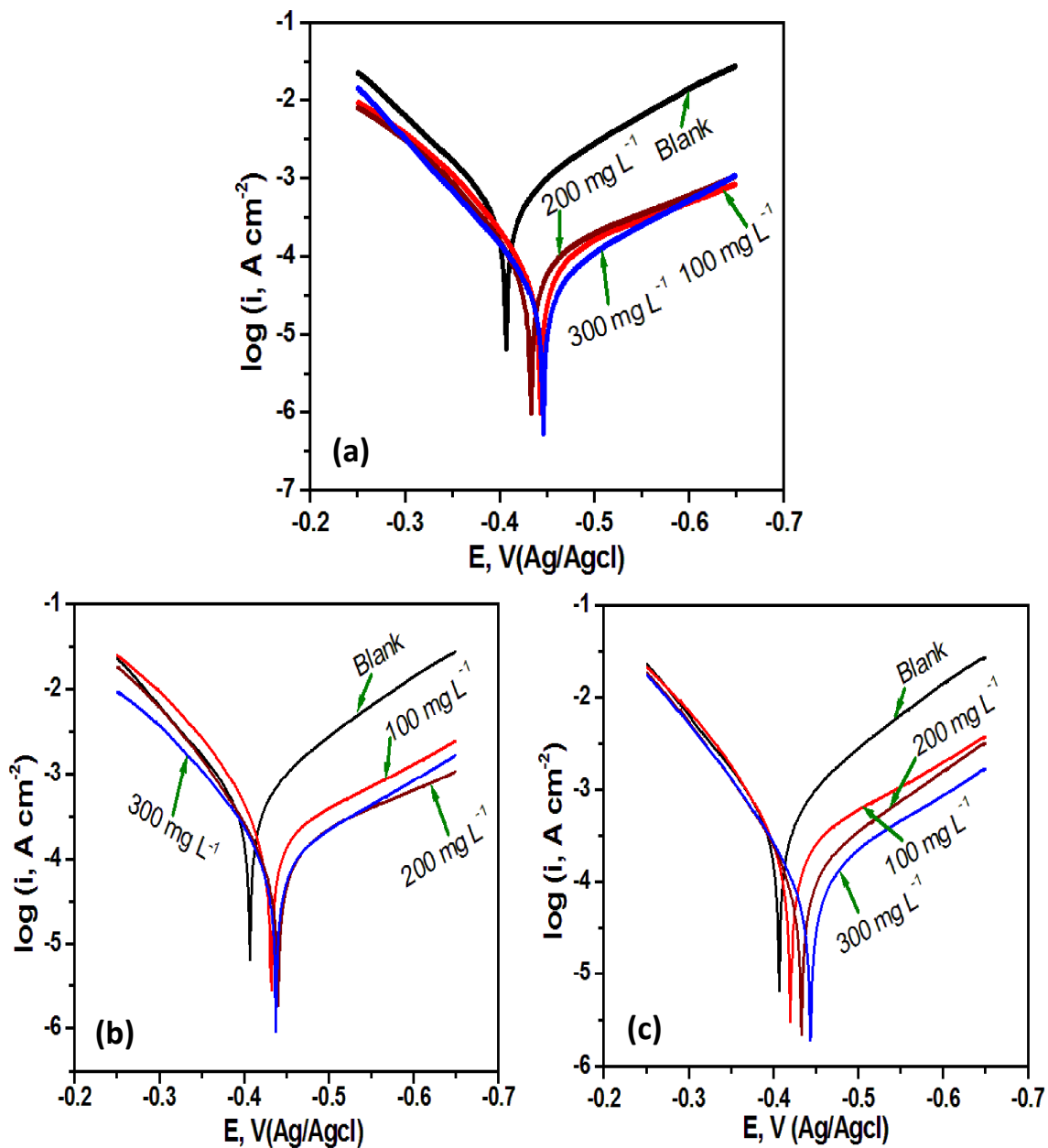


**Figure 5.12** Tafel polarization curves for mild steel with different concentrations of (a) RMPPE, (b) RIMPPE, and (c) ORIMPPE in 1 M HCl.

**Table 5.3 Tafel parameters of mild steel corrosion in 1 M HCl with different concentration of inhibitor at RT.**

Type of extract	Conc. of inhibitor (mg L <sup>-1</sup> )	-E <sub>corr</sub> (mV)	I <sub>corr</sub> (μA cm <sup>-2</sup> )	b <sub>a</sub> (mVdec <sup>-1</sup> )	b <sub>c</sub> (mVdec <sup>-1</sup> )	μ <sub>p</sub> %	L <sub>PR</sub> (Ω cm <sup>2</sup> )	μ <sub>PR</sub> %
	Blank	408	498	115	78	-	45	-
<b>Raw</b>	100	443	93	123	49	81	255	82
	200	433	71	124	51	86	294	85
	300	446	48	131	68	90	448	90
<b>Ripe</b>	100	432	164	117	52	67	127	65
	200	440	111	135	48	78	196	77
	300	437	88	114	58	82	221	80
<b>Over ripe</b>	100	420	196	121	52	61	110	59
	200	433	128	126	67	74	174	74
	300	443	114	128	60	77	208	78

Technical parameters of electrochemical corrosion, such as, E<sub>corr</sub>, I<sub>corr</sub>, slope of anodic (b<sub>a</sub>) and cathodic (b<sub>c</sub>) polarization curves and linear polarization resistance values were determined from the curves obtained in both acid media, and listed in Table 13. Through investigation of various parameters it was revealed that E<sub>corr</sub> of corrosion reactions displaced in presence of the extracts; however, the direction of displacement in E<sub>corr</sub> values showed a random pattern. A maximum shift of 38 mV, 32 mV and 35 mV with respect to uninhibited mild steel was acknowledged in HCl in presence of RMPPE,

RIMPPE and ORIMPPE, respectively. On the other hand, a maximum displacement of 14, 2 and 1 mV was achieved in  $H_2SO_4$  in presence of respective inhibitor (Table 14). This information suggested that banana peel extracts worked as a mixed type inhibitor in acid media. Because, the maximum change in  $E_{corr}$  values in either positive or negative direction were less than 85 mV. Furthermore, slope of anodic and cathodic polarization curves ( $b_a$  and  $b_c$ ) varied with ripening of the peels and concentration of inhibitor; however, the changes were not observed to follow any certain trend. This fact supported the conclusion of  $E_{corr}$  values analysis, i.e., inhibitor suppressed both cathodic and anodic partial reactions.

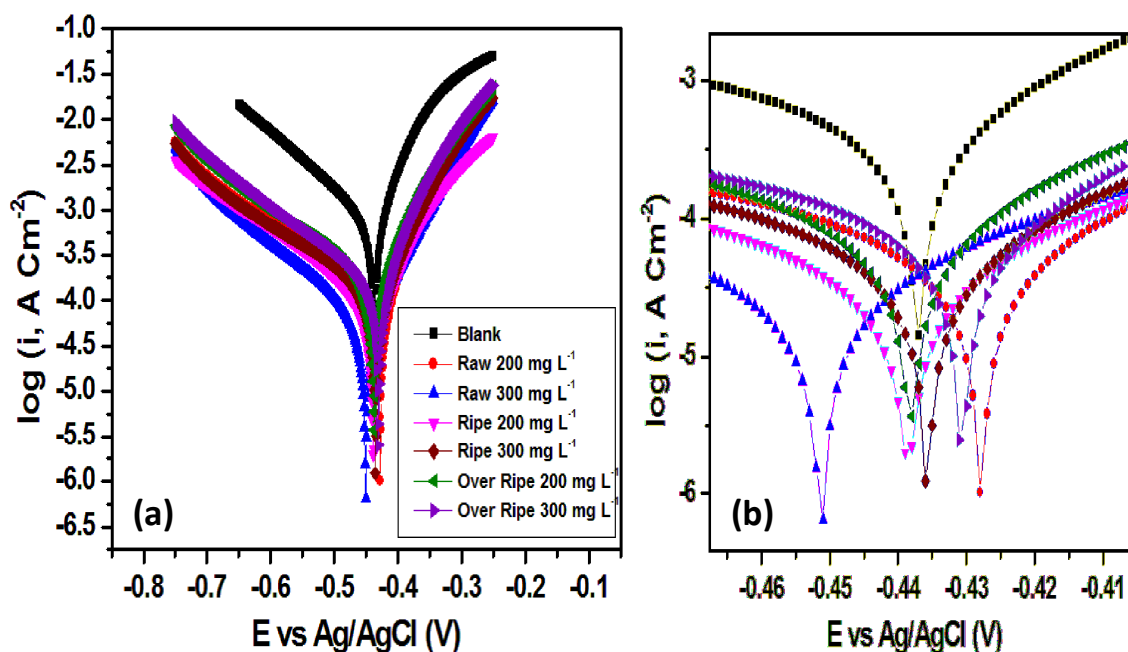


**Figure 5.13 (a) Tafel polarization curves for mild steel with different concentrations of RMPPE, RIMPPE, and ORIMPPE in 0.5 M  $H_2SO_4$  (b) Zoom view of the curves**

It was also noticed from Table 13 and 14 that corrosion current retarded as a function of inhibitor concentration, which suggested that corrosion rates of mild steel samples in HCl and  $H_2SO_4$  solutions were slowed down by inhibitor. Perhaps, the organic matters of banana peel extracts modified mild steel electrode by getting adsorbed on metal surface,

which caused lowering in corrosion current values. This explanation of corrosion inhibition could be done on the basis of polarization resistance values that increased with the inhibitor concentration.

**Table 5.4 Tafel parameters of mild steel corrosion in 0.5 M H<sub>2</sub>SO<sub>4</sub> with different concentration of inhibitor at RT.**

Maturity of extract	Conc. of inhibitor (mg L <sup>-1</sup> )	-E <sub>corr</sub> (mV)	I <sub>corr</sub> (μA cm <sup>-2</sup> )	b <sub>a</sub> (mV dec <sup>-1</sup> )	b <sub>c</sub> (mV dec <sup>-1</sup> )	μ <sub>p</sub> %	L <sub>p</sub> (Ω cm <sup>2</sup> )	μ <sub>PR</sub> %
	Blank	<b>437</b>	<b>647</b>	<b>98</b>	<b>64</b>	-	<b>26</b>	-
<b>Raw</b>	200	428	120	132	51	81	144	82
	300	451	81	139	57	87	193	86
<b>Ripe</b>	200	439	184	115	59	71	98	73
	300	436	136	134	47	79	132	80
<b>Over ripe</b>	200	431	214	127	50	66	74	65
	300	438	181	120	47	72	102	74

#### 5.4 Electrochemical Impedance Spectroscopy

Impedance spectra for mild steel test samples in 1 M HCl and 0.5 M H<sub>2</sub>SO<sub>4</sub> solutions with and without banana peels extracts are shown in Figure 54. Through inspection of Nyquist plots it could be observed that impedance spectra were in a shape of depressed semi circles, which indicated formation of a modified capacitive layer of organic molecules of the extracts at metal-acid interface [Fawcett et al. 1992]. Figure 54 revealed that the diameters of these semicircles were increasing with the increasing concentration

of inhibitor. This observation suggested that the charge transfer reactions were inhibited by banana peel extracts. However, maximum increase in charge transfer resistance with the extract concentration in both acid media was acknowledged for RMPPE followed by RIMPPE and ORIMPPE.

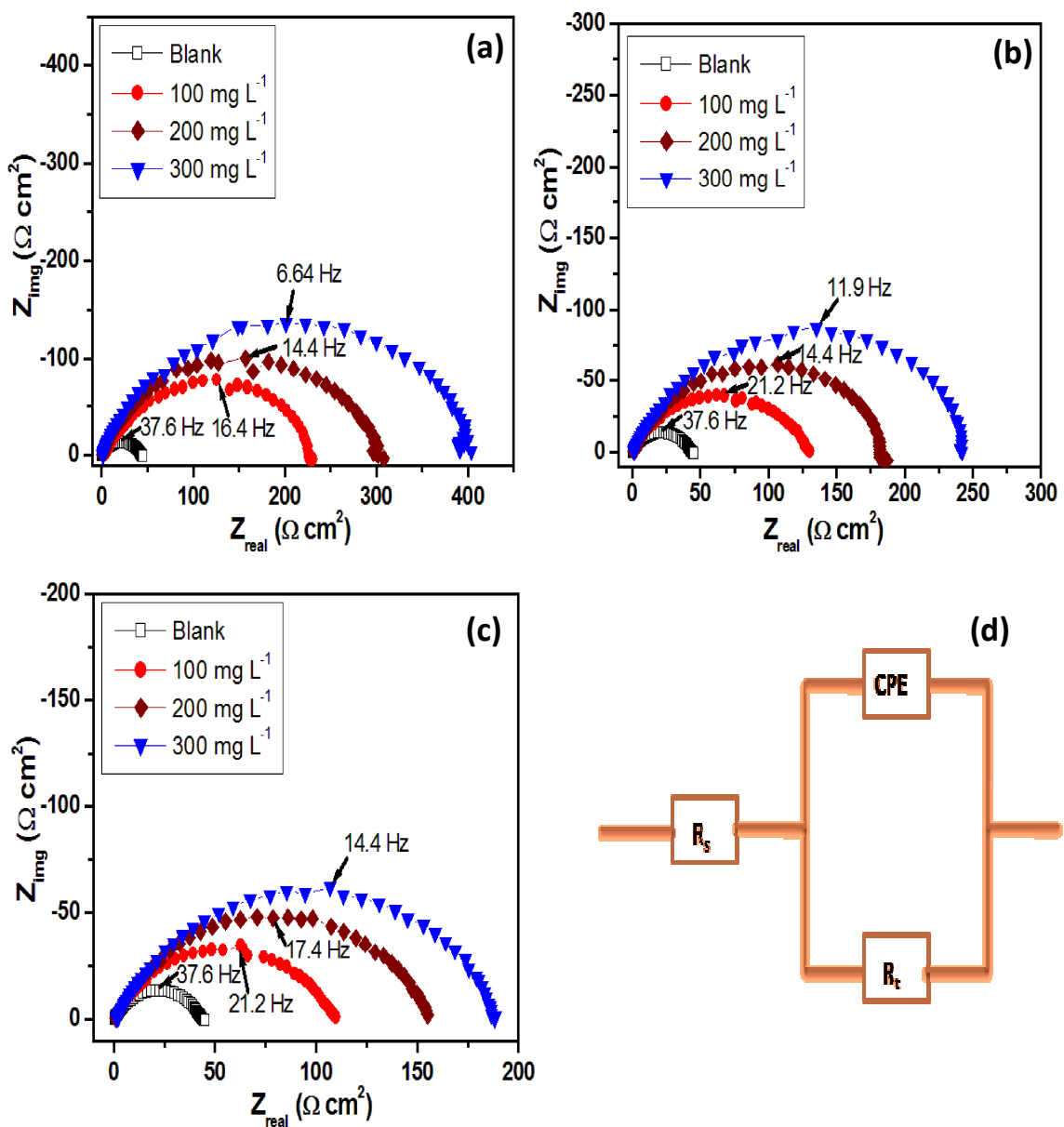


**Figure 5.14** Nyquist plots for mild steel in 1 M HCl in presence of (a) raw, (b) ripe, and (c) over ripe banana peels extracts. (d) Equivalent electrochemical circuit for simulation of the experimental results.

To simulate the results of EIS, we have used an equivalent electrochemical circuit (shown in Figure 54d) and determined various parameters like solution resistance  $R_s$ , charge transfer resistance  $R_t$ , double layer capacitance  $C_{dl}$ , and magnitude of constant phase element (CPE)  $Y_0$ , which are listed in Table 15.

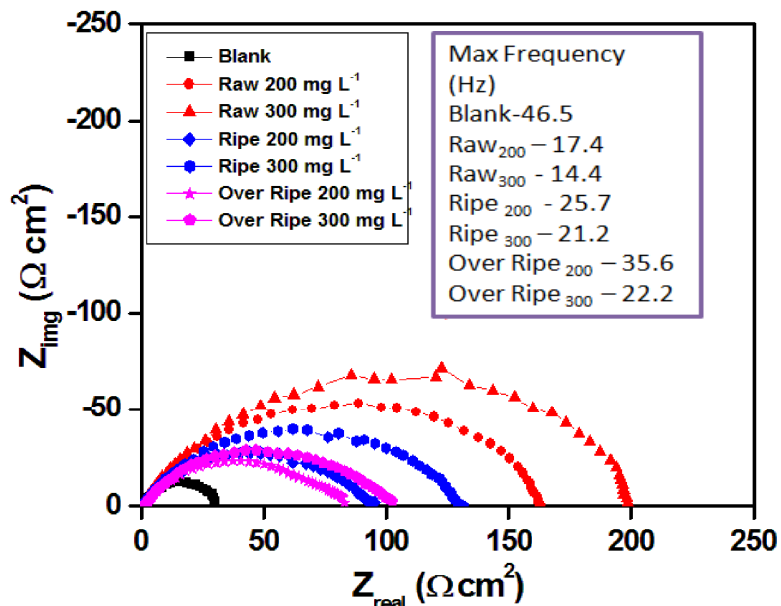


**Figure 5.15** Nyquist plots for mild steel in 0.5 M H<sub>2</sub>SO<sub>4</sub> in presence of banana peel extracts at room temperature.

EIS results (Table 15 and 16) revealed that charge transfer resistances  $R_t$  in both acid media increased with the inhibitor concentration, while  $C_{dl}$  values were found decreased with increase in the extract concentration. The maximum value of corrosion resistance was acknowledged at 300 mg L<sup>-1</sup> concentration of banana peel extracts in both HCl and H<sub>2</sub>SO<sub>4</sub> solutions. The values for raw banana peel extract in 1 M HCl and 0.5 M H<sub>2</sub>SO<sub>4</sub> were 396 and 204 Ω cm<sup>2</sup> respectively, while they were 241 & 130 Ω cm<sup>2</sup> and 187 & 104 Ω cm<sup>2</sup> for ripe and over ripe banana peel extract, respectively. A sudden increase in charge transfer resistance values in presence of inhibitor could be attributed to adsorption of organic molecules of the extracts on metal surface. Due to that, movement of charges across the interface was successfully blocked and corrosion inhibition was achieved

[Yadav et al, 2013]. This statement was well supported by  $C_{dl}$  values, which could be better explained with the help of Helmholtz equation (Eqn. 25). It is evident from the equation that the value of double layer capacitance is directly dependent of local dielectric constant of formed film  $\epsilon$ , dielectric constant of free space  $\epsilon_0$  and exposure area  $A$ , while posses an opposite relation with thickness of layer formed at the interface  $t$ . Accordingly, decrease in  $C_{dl}$  values with increase in inhibitor concentration indicated that either thickness of inhibitive layer increased or local dielectric constant of film decreased, or both occurred simultaneously.

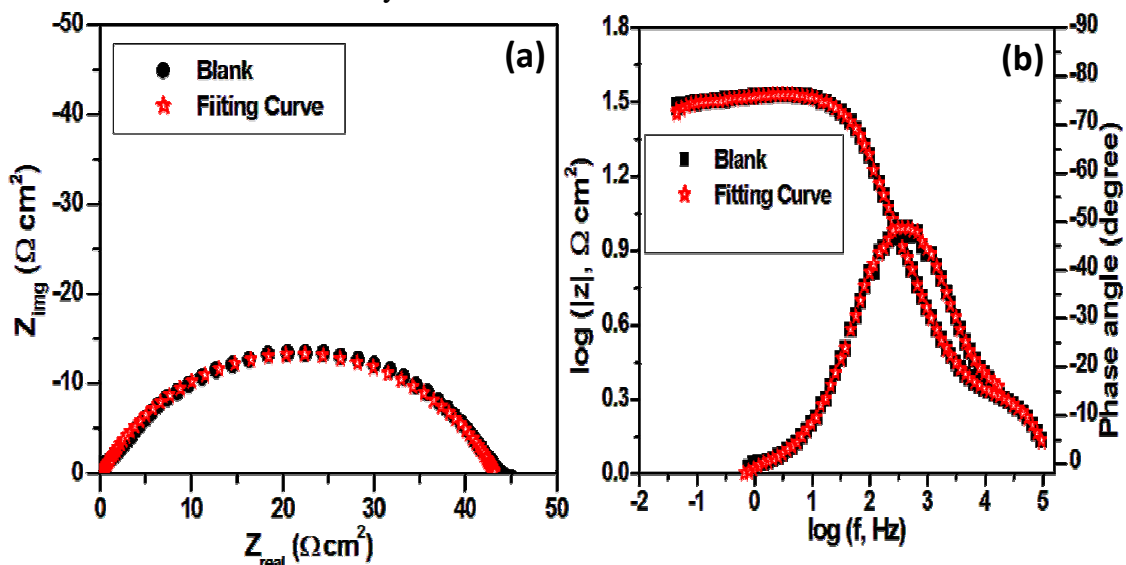


**Figure 5.16 Nyquist plots and bode plots showing relation between experimental and simulated results.**

The value of  $n$  is an important physical parameter and reflects microscopic changes occurring on the metal surface. We have also monitored this technical parameter to show the effect of inhibitor on mild steel corrosion (Table 15 and 16). The  $n$  value of 0.7022 and 0.7220 was achieved for mild steel in HCl and H<sub>2</sub>SO<sub>4</sub> solution, which was significantly changed with increase in inhibitor concentration. According to equation 23, it is obvious that if (1)  $n=0$ , electrical circuit will show the characteristics of a pure

resistor having magnitude of  $Y^{-1}$ , (2)  $n=1$ , the circuit will have the characteristics of a pure capacitor with magnitude of  $C$ , and (3)  $n=-1$ , circuit will correspond to a pure inductor with magnitude of  $Y^{-1}$  [J.R. Macdonald, 1987]. In view of above facts, it could be stated that increase in  $n$  values reflected capacitive behavior of mild steel in HCl and  $H_2SO_4$  solution in presence of the extracts. However, in any case the value of  $n$  is found less than 1, which meant that mild steel did not show ideal capacitor behavior in either solution. The reason might be arbitrary distribution of current on electrode surface or irregularity of electrode surface, creating frequency fluctuation.

**Table 5.5 Technical Parameters obtained from Nyquist Plots at different concentration of inhibitor for mild steel in 1 M HCl at RT.**

Maturity of banana peel extract	Conc. of inhibitor	$R_s$ ( $\Omega\text{ cm}^2$ )	$R_t$ ( $\Omega\text{ cm}^2$ )	$n$	$Y_0$ ( $10^{-6}\Omega^{-1}\text{ cm}^{-2}$ )	$C_{dl}$ ( $\mu\text{F cm}^{-2}$ )	$\mu_{Rt}$ %
	<b>Blank</b>	<b>0.25</b>	<b>43</b>	<b>0.7022</b>	<b>473</b>	<b>91.5</b>	<b>-</b>
<b>Raw</b>	100 mg L <sup>-1</sup>	1.66	227	0.7151	158	42.0	81
	200 mg L <sup>-1</sup>	0.96	298	0.7768	098	35.5	86
	300 mg L <sup>-1</sup>	1.01	<b>396</b>	0.7802	086	<b>33.1</b>	89
<b>Ripe</b>	100 mg L <sup>-1</sup>	0.94	128	0.7339	210	57.0	66
	200 mg L <sup>-1</sup>	1.12	182	0.7476	165	50.5	76
	300 mg L <sup>-1</sup>	1.09	<b>241</b>	0.7577	144	<b>41.4</b>	82
<b>Over Ripe</b>	100 mg L <sup>-1</sup>	1.02	109	0.7185	305	80.5	61
	200 mg L <sup>-1</sup>	0.94	155	0.7382	184	52.1	72
	300 mg L <sup>-1</sup>	1.46	<b>187</b>	0.7402	167	<b>49.4</b>	77

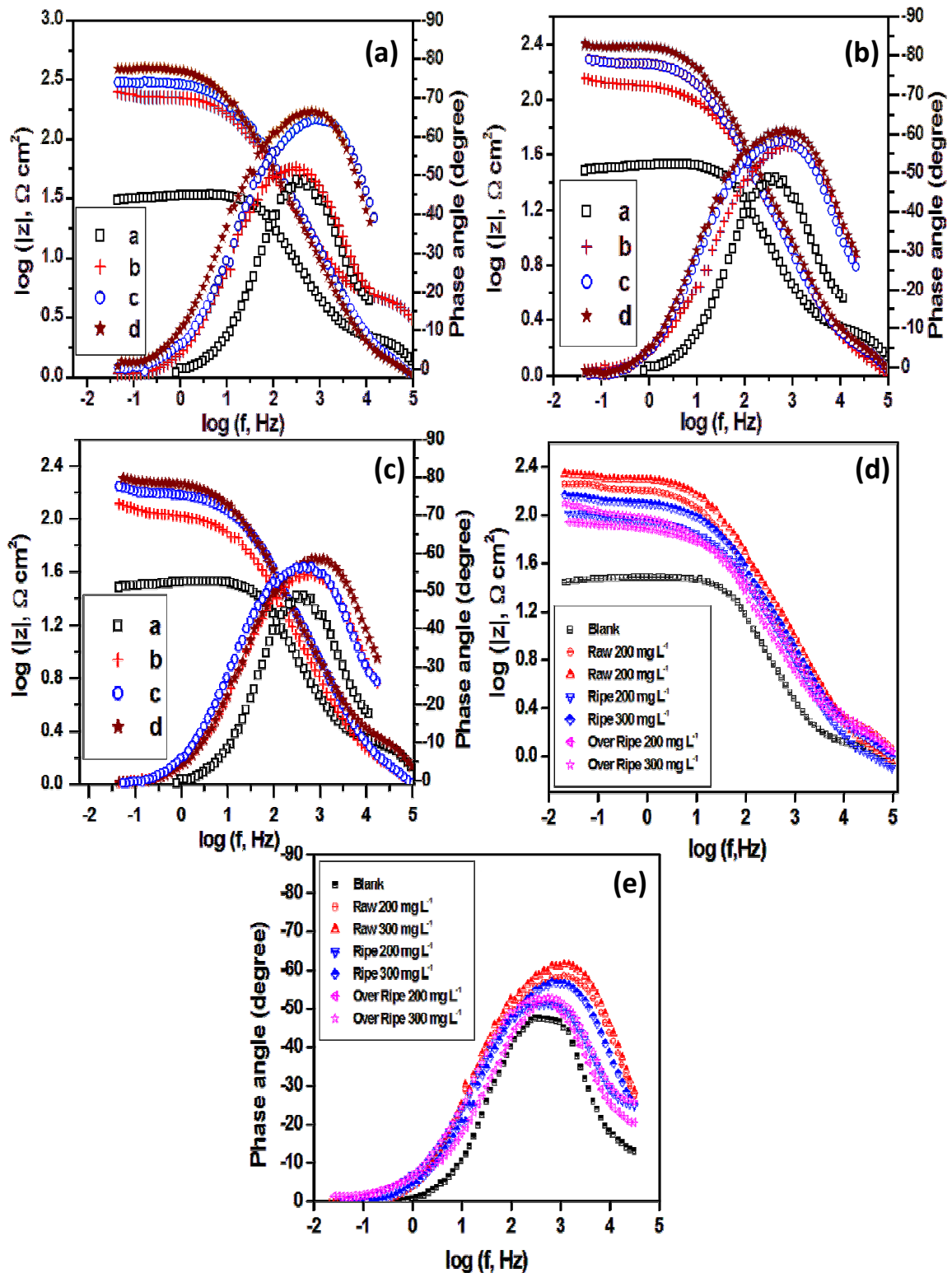


Figure 5.17 Bode plots for mild steel without and with different concentration of (a) raw, (b) ripe, and (c) over ripe banana peel extracts. (d) and (e) Bode plots for banana peel extracts in  $0.5 \text{ M H}_2\text{SO}_4$ .

The similar information was known via bode plots (Figure 57). A hostile attack of hydrochloric acid and sulfuric acid damaged mild steel enormously as well as increased surface irregularity. The same could be easily detected by low phase angle in bode plots of blank solutions (Figure 57). In contrast, organic matters of the extracts adsorbed on metal and successfully decreased irregularities of mild steel surface, causing increase in phase angle. However, the characteristics of a pure capacitor were not noticed in bode plots (Phase angle  $< 90^\circ$ ), which was in good agreement with the n values.

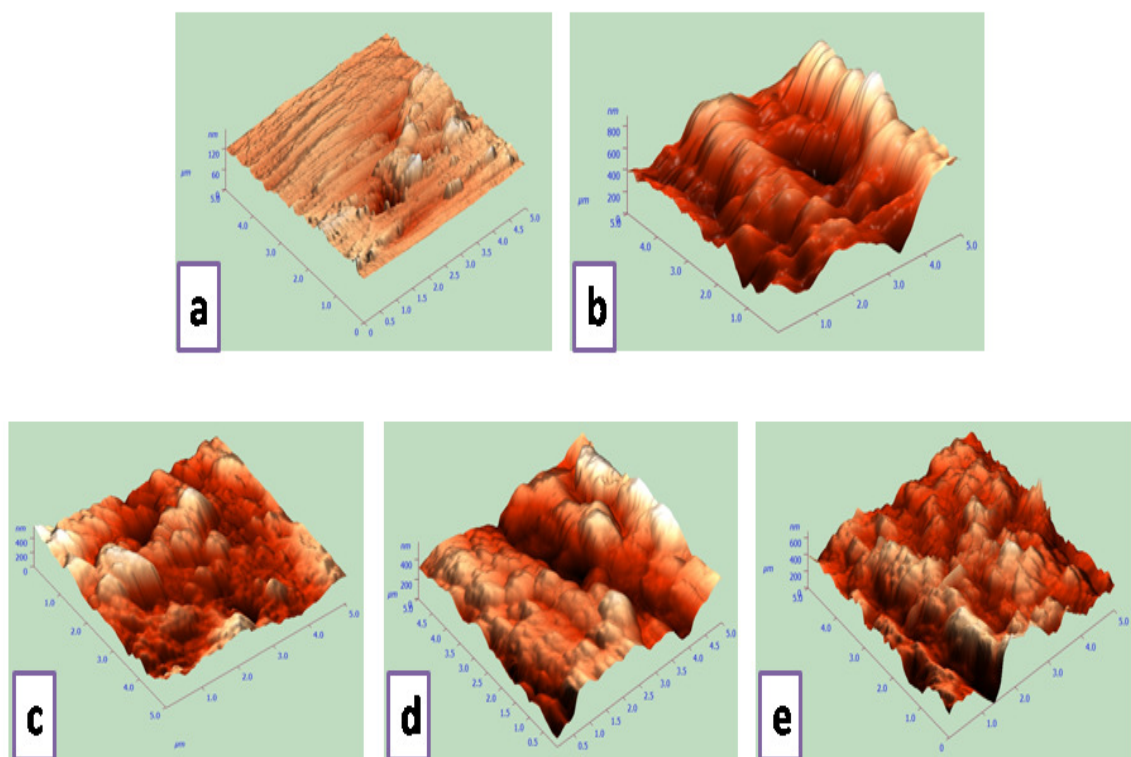
**Table 5.6 Corrosion parameters obtained from Nyquist Plots for mild steel in 0.5 M H<sub>2</sub>SO<sub>4</sub> with different concentration of the extracts at RT.**

Type of extract	Conc. of inhibitor	R <sub>s</sub> ( $\Omega \text{ cm}^2$ )	R <sub>t</sub> ( $\Omega \text{ cm}^2$ )	n	Y <sub>0</sub> ( $10^{-6} \Omega^{-1} \text{ cm}^{-2}$ )	C <sub>dl</sub> ( $\mu\text{F cm}^{-2}$ )	$\mu_{Rt}$ %
	<b>Blank</b>	<b>0.95</b>	<b>30.6</b>	<b>0.7220</b>	<b>505</b>	<b>100.6</b>	<b>-</b>
<b>Raw</b>	200 mg L <sup>-1</sup>	1.22	170.3	0.7320	202	58.7	<b>82</b>
	300 mg L <sup>-1</sup>	0.86	204.0	0.7650	130	42.0	<b>85</b>
<b>Ripe</b>	200 mg L <sup>-1</sup>	0.78	96.0	0.7351	239	61.0	<b>69</b>
	300 mg L <sup>-1</sup>	0.95	130.8	0.7360	214	58.8	<b>77</b>
<b>O. Ripe</b>	200 mg L <sup>-1</sup>	1.07	82.1	0.7005	361	78.6	<b>63</b>
	300 mg L <sup>-1</sup>	1.15	104	0.7060	314	75.1	71

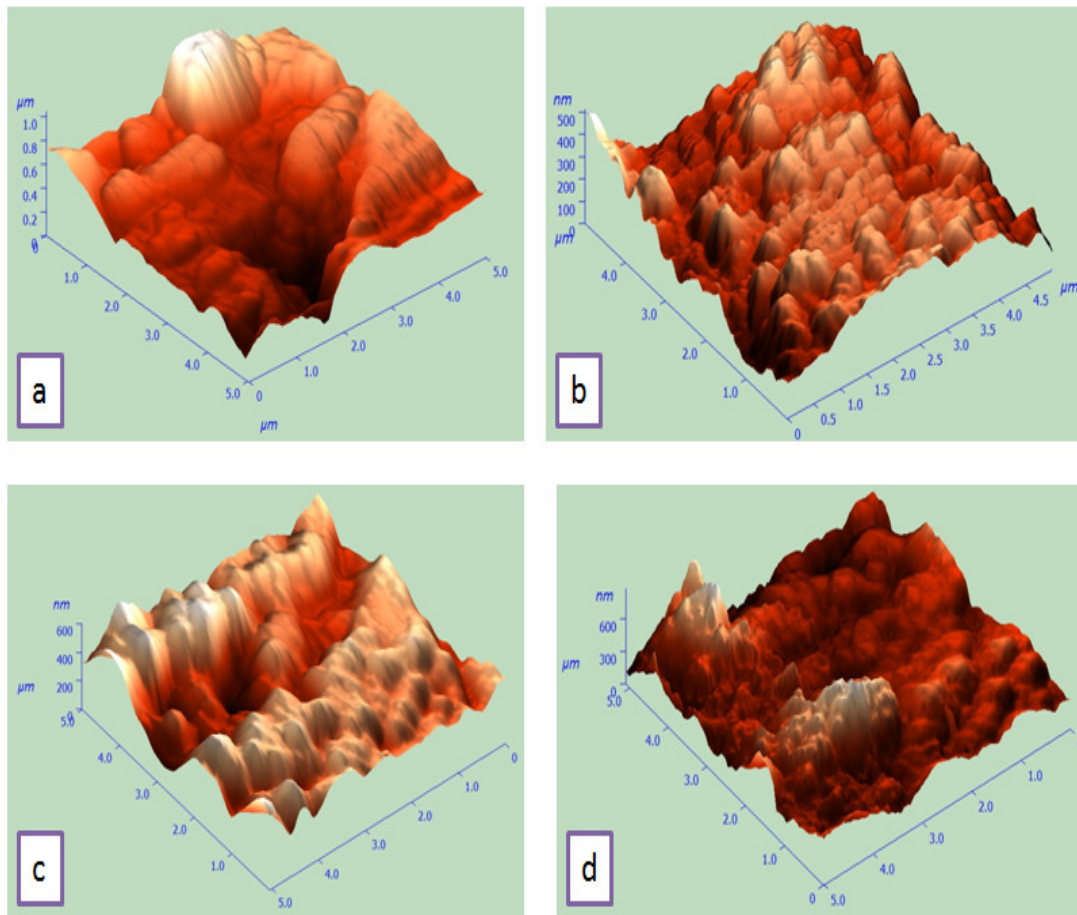
### 5.5 Surface Analysis

Figure 58 and 59 demonstrates surface morphology changes of mild steel samples with the type of acid and banana peel extracts. Figure 58a shows few holes and hilly area on the metal surface as well as scratches spots, which was appeared on the surface due to

uneven polishing of the test specimens during sample preparation process. The average roughness of mild steel sample before immersion in acid solutions was determined as 16 nm. After immersion of test sample in acid media a violent reaction took place between mild steel and acid media, and the surface roughness was drastically increased to 116 nm and 171 nm in HCl and H<sub>2</sub>SO<sub>4</sub> respectively (Figure 58 b and 59 a). On the other side, the chemical constituents of the extracts effectively maintained the surface homogeneity by getting adsorbed over mild steel surface (Figure 58c to e and Figure 59 b to d). An average roughness of 54 nm and 72 nm, 71 nm and 86 nm, and 78 nm and 92 nm was achieved using raw, ripe, and over ripe banana peel extract respectively in HCl and H<sub>2</sub>SO<sub>4</sub> solutions.



**Figure 5.18** 3D AFM images of mild steel (a) prepared, (b) corroded in 1 M HCl, (c) inhibited by RMPPE, (d) inhibited by RIMPPE and (e) inhibited by ORIMPPE



**Figure 5.19** 3D AFM images of mild steel (a) corroded in 0.5 M H<sub>2</sub>SO<sub>4</sub>, (b) inhibited by RMPPE, (c) inhibited by RIMPPE and (d) inhibited by ORIMPPE

The similar information was known by surface morphological study by SEM (Figure 60). In acid solutions, mild steel corroded very fast and the surface became highly rough and irregular, which showed intensity of acid attack. On the other side, mild steel corrosion was successfully inhibited by the extracts (Figure 60 d-i) ; however, better corrosion inhibition effects were visualized in HCl than in H<sub>2</sub>SO<sub>4</sub> solution. Thus, it could be stated on the basis of morphological study of mild steel in presence and absence of inhibitor that banana peel extract efficiently inhibited mild steel corrosion in HCl and H<sub>2</sub>SO<sub>4</sub> solutions.

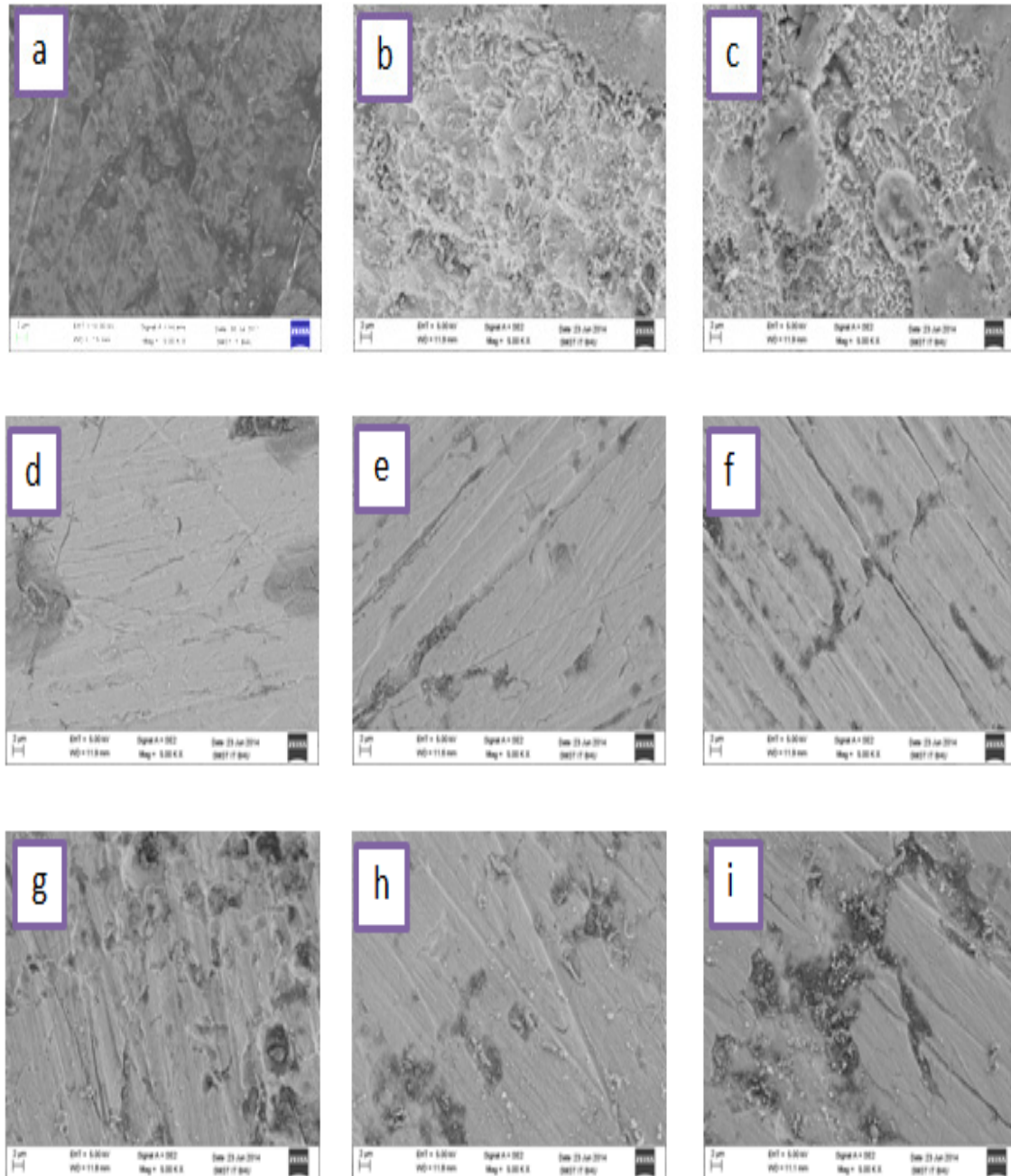


**Figure 5.20** SEM images of (a) mild steel, (b) corroded sample in 1 M HCl, (c) corroded sample in 0.5 M H<sub>2</sub>SO<sub>4</sub>, (d) & (e) inhibited by raw extract in HCl and H<sub>2</sub>SO<sub>4</sub>, (f) & (g) inhibited by ripe extract in HCl and H<sub>2</sub>SO<sub>4</sub> and (h) & (i) inhibited by ripe extract in HCl and H<sub>2</sub>SO<sub>4</sub> solutions.

### 5.6 Mechanism of Corrosion Inhibition

Banana peels are a rich source of nutrients and various bioactive molecules [Sundaram et al., 2011; Kanazawa and Sakakibara, 2000], such as, gallic acid, catechin, dopamine, ascorbate, etc. Among all, gallic acid is a major organic compound of the peels. This fact was authenticated by HPLC chromatogram as well as by UV-visible and FTIR study. Hence, it can be stated here that inhibition potential of banana peel extracts mainly depends on the inhibitive properties of gallic acid.

From a careful analysis of the results obtained by the employed techniques, it could be highlighted that corrosion inhibition of mild steel in acid media was achieved due to effective blanketing of the surface by adsorbed organic molecules of the extracts. Hence, it could be extracted from above mentioned fact that corrosion inhibition mechanism is an adsorption mechanism in real. Accordingly, adsorption mechanism of the extracts on mild steel surface should be investigated. Figure 61 illustrates a schematic arrangement that indicate the possible interaction ways between mild steel and inhibitors.

In the adsorption process, the nature of charge on metal surface plays an important role. Hence, we are forced to find net charge accumulation on mild steel surface. To determine the total charge on steel surface, we used following equation;  $E_{tot} = E_{corr} - E_{q=0}$ , where  $E_{q=0}$  is used to denote zero charge potential. In our case,  $E_{corr}$  value of iron in 1 M HCl and 0.5  $H_2SO_4$  was achieved as -408 mV and -437 mV vs Ag/AgCl electrode, respectively. This fact suggested that mild steel surface carried positive charges in its surface in both acid media ( $E_{tot} = -408 - (-485) = 77$  mV (HCl),  $E_{tot} = -437 - (-505) = 68$  mV ( $H_2SO_4$ )). It is evident from zero charge potential calculation that mild steel was more positively

charged in hydrochloric acid than in sulfuric acid, which itself explain the reason of greater inhibition efficiency in HCl with respect to H<sub>2</sub>SO<sub>4</sub>.

The organic moieties of banana peel extracts, primarily gallic acid, have ability to get protonized in acid media. These charged species may form a physical bonding with metal surface via electrostatic interactions, as illustrated in Figure 61. Furthermore, gallic acid like molecule contains benzene rings (source of  $\pi$  electrons) and hetero atoms (in this case oxygen as source of non bonding electrons) in its chemical structure. These unsaturated electrons could start the formation of chemical bonding between metal and adsorbed molecules on the surface (vacant d-orbital electrons of iron). Undergoing the same process, other organic molecules of the extracts might adsorb on mild steel. Thus, adsorption of molecules formed an inhibitive layer on metal surface and hence corrosion inhibition of mild steel was acknowledged.

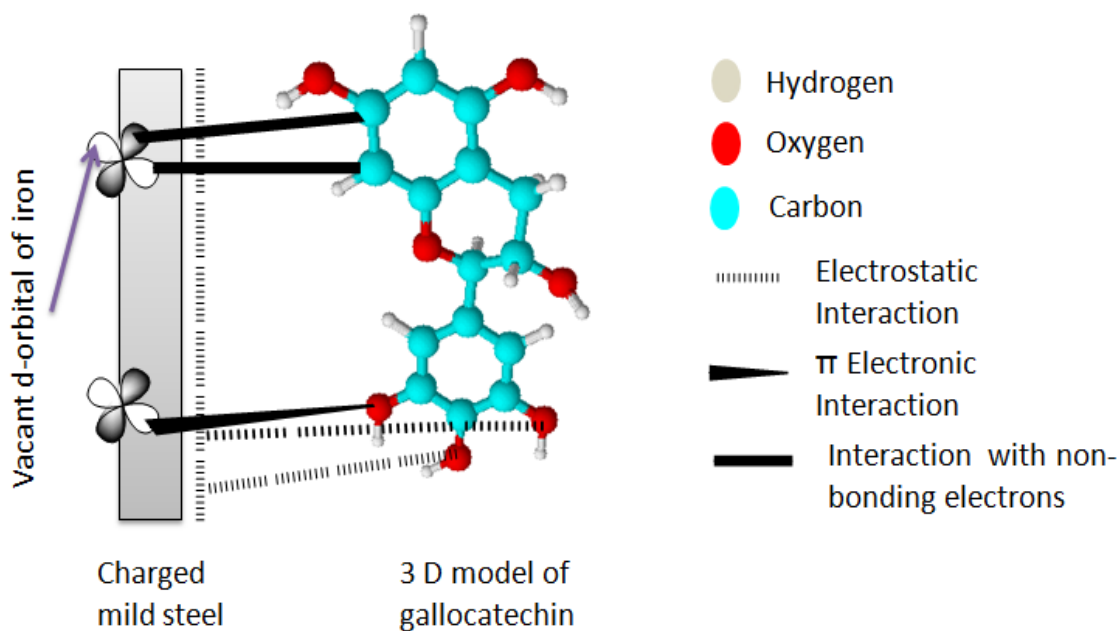


**Figure 5.21 Schematic explanation of corrosion inhibition activity of banana peel extracts**